




Jardim do Seridó Suite: first example of Ediacaran peraluminous magmatism in the Rio Piranhas-Seridó Domain, Borborema Province, Northeast Brazil

Izaac Cabral Neto¹ , Vladimir Cruz de Medeiros¹, Rogério Cavalcante¹, Priscila Rezende Fernandes², Francisco Valdir Silveira¹, Elton Luiz Dantas³, Joseneusa Brilhante Rodrigues⁴, Ioná Cunha⁵, Vinicius Jose de Castro Paes⁶, Luana Duarte Santos⁶, Ivana Conceição Araújo Pinho⁷

¹CPRM-Serviço Geológico do Brasil (NANA/SUREG-RE), Rua Professor Antonio Henrique de Melo, 2010, Natal-RN, Brazil, CEP: 59078-580

²CPRM-Serviço Geológico do Brasil (GEREMI/SUREG-RE) Recife, Brazil

³UnB – Universidade de Brasília, Instituto de Geociências, Brasília, Brazil

⁴CPRM-Serviço Geológico do Brasil (SEDE), Brasília, Brazil

⁵CPRM-Serviço Geológico do Brasil (DIPEME/SUREG-SA), Salvador, Brazil

⁶CPRM-Serviço Geológico do Brasil (GEREMI/SUREG-BH), Belo Horizonte, Brazil

⁷CPRM-Serviço Geológico do Brasil (GEREMI/SUREG-SA), Salvador, Brazil

Abstract

Peraluminous granitoids were recently mapped in the Rio Piranhas-Seridó Domain, the northeast portion of the Borborema Province. These bodies occur as stock and intrusive dikes in the metapelites of the Seridó Formation, constituting the Jardim do Seridó Suite. This suite has two facies. The first and most expressive facies consists of a medium-grained and whitish leucocratic monzogranite with muscovite, garnet, and biotite, while the second is represented by fine-grained and greyish leucocratic granodiorites with biotite, cropping out mainly on the edges of the main body. The thermobarometric conditions for the crystallization of the monzogranites were estimated between 2-5 kbar and 690-950 °C, whereas the lithochemical data indicate a syn-collisional peraluminous signature. Neoproterozoic garnet-biotite schist xenoliths of the Seridó Formation are sometimes observed partially assimilated in the main body (stock). A U-Pb zircon age of 592 ± 2 Ma obtained in the main body is considered as the crystallization age of the Jardim do Seridó Suite, corroborating the proposed existence of peraluminous magmas associated with the Brasiliano Orogenesis in the Rio Piranhas-Seridó Domain. The chemical and petrographic data identified this suite as fertile to that it can generate dikes of rare elements-bearing pegmatites.

Article Information

Publication type: Research paper

Submitted: 26 February 2019

Accept: 21 June 2019

On line pub: 25 July 2019

Editor: Evandro Klein

Keywords:

Peraluminous magmatism
two-mica granite
Rio Piranhas-Seridó Domain
Borborema Province
Ediacaran

*Corresponding author

Izaac Cabral Neto

E-mail address:

izaac.cabralneto@cprm.gov.br

1. Introduction

The Rio Piranhas-Seridó Domain (DPS) of the Borborema Province is marked by significant Ediacaran-Cambrian magmatism that is represented by several batholiths, stocks, and dikes. Based on the petrographic, geochemical and geochronological data, Nascimento et al. (2015) grouped the granite bodies of this domain into six suites: Shoshonitic, Porphyritic high-K Calc-Alkaline, Equigranular high-K Calc-Alkaline, Calc-Alkaline, Alkaline, and Charnockite Alkaline, characterized as metaluminous or weakly peraluminous.

Recently, Cabral Neto et al. and Souza et al. (2018) identified and mapped leucocratic granitoids bearing muscovite, garnet and biotite in the region just south of Jardim do Seridó, in Rio Grande do Norte state. These intrusive bodies comprise the first records of peraluminous Ediacaran granite-granodiorites in the DPS, located in the same tectonic-geological context

of important deposits and mineral occurrences (e.g., gold, tungsten, iron, Sn, Be, Li, Ta-Nb and Ta).

This work presents the field correlations, petrographic, geochemical and geochronological data of the peraluminous Ediacaran granite-granodiorites in the DPS, discussing the possible tectonic environment in which they formed and their fertility for rare elements, such as Ta, Be, Li, Cs, Nb, and Rb.

2. Geological context

2.1. Regional Geology

The Borborema Province covers the extensive geological-structural domain located in northeastern Brazil that was consolidated in the Brasiliano/Pan-African Cycle (Almeida et al. 1977, 1981; Jardim de Sá et al. 1992). Its boundaries are defined by the São Francisco Craton (Archaean to



Paleoproterozoic) to the south, the Parnaíba Basin (Paleozoic to Mesozoic) to the west, and by the Meso-Cenozoic sedimentary basins of the Brazilian continental margin to the north and east (Figure 1).

Over the years, different authors (Brito Neves 1975, 1983; Almeida et al. 1977; Santos and Brito Neves 1984; Jardim de Sá et al. 1988; Caby et al. 1991; Jardim de Sá et al. 1992; Jardim de Sá 1994; Van Schmus et al. 1995; Santos 1996; Brito Neves et al. 2000; Santos et al. 2000) presented several proposals for the compartmentalization of this province based on several concepts, including that of terrains and/or tectonostratigraphic domains. Medeiros et al. (2017) subdivided the province into nine domains: Médio Coreau, Ceará Central, Jaguaribeano, Rio Piranhas-Seridó, São José do Campestre, Zona Transversal, Pernambuco-Alagoas, Sergipano, and Riacho do Pontal (Figure 1).

In this context, the study site is located in the Brasiliano-age Rio Piranhas-Seridó Domain (DPS) bordering the Picuí-João Câmara, Portalegre and Patos shear zones to the east, west, and south, respectively, while the northern boundary is covered by the Mesozoic and Cenozoic sediments of the Potiguar Basin (Figure 2).

The DPS region consists of Paleoproterozoic units, referred to in the bibliography as the Arabia Complex (Costa and Dantas 2014), Caicó Complex (Jardim de Sá 1984; Dantas 1988; Souza 1991; Jardim de Sá 1994; Brito Neves et al. 2000; Souza et al. 2007, 2016) and Rhyacian augen gneiss (Hollanda et al. 2011; Medeiros et al. 2012), besides the Neoproterozoic metamorphosed supracrustal rocks of the Seridó Group (Jardim de Sá and Salim 1980; Jardim de Sá 1984, 1994; Van Schmus et al. 2003; Hollanda et al. 2015) and Ediacaran-Cambrian granitoids (Nascimento et al. 2015),

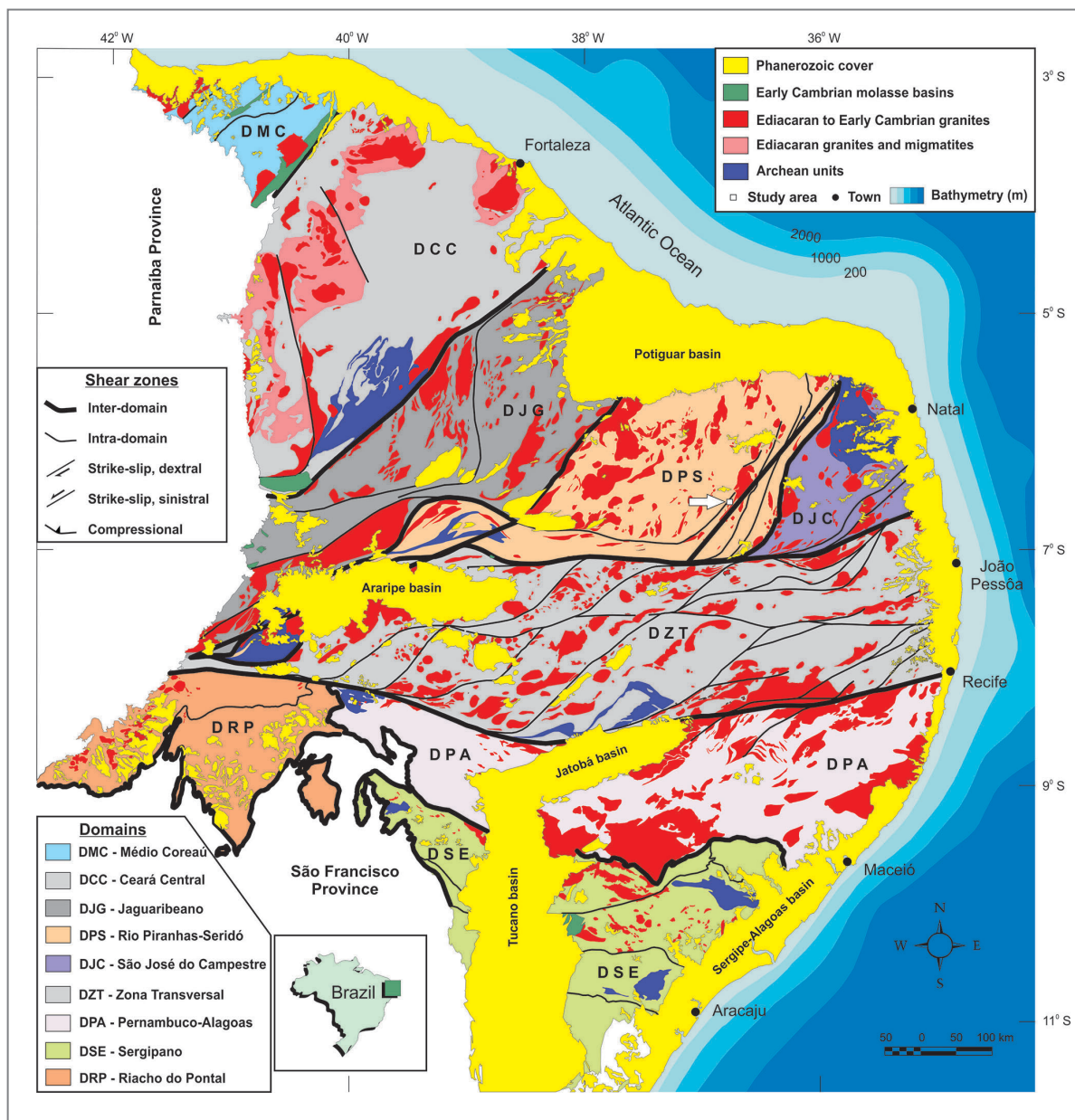


FIGURE 1 – Tectonostratigraphic domains of the Borborema Province according to Medeiros et al. (2017), with the location of the study area (white arrow).

as shown in Figure 2 and summarized in Table 1. Locally, Archean rocks occur in the regions of Bonfim/Lajes (Dantas et al. 2014) and São Tomé (Ruiz et al. 2018), which comprise the Amarante Complex (Figure 2, Table 1), and Saquinho (Cavalcante et al. 2018).

From the base to the top, the Seridó group consists of the Jucurutu (paragneisses with intercalations of marbles, calc-silicate rocks, mica schist, metavolcanic and iron formations), Equador (quartzites and metaconglomerates) and Seridó (predominant mica schist with rare intercalations of metavolcanic, marbles and calc-silicate rocks) formations, as proposed by Jardim de Sa and Salim (1980), Jardim de Sá (1984, 1994), Medeiros et al. (2017), and Cavalcante et al. (2018). U-Pb zircon dating indicates sedimentation ages between 650 and 610 Ma for the Seridó and Jucurutu formations (Van Schmus et al. 2003; Hollanda et al. 2015). The DPS is intruded by several granitoid bodies dated between 599 and 527 Ma reviewed by Nascimento et al. (2015) and summarized below.

Nearby the study region, the occurring Brasiliano granitoids of the São João do Sabugi, Itaporanga and Dona Inês types (Angelim et al. 2006) have been classified as Shoshonitic, Porphyritic high-K Calc-Alkaline, Equigranular high-K Calc-Alkaline, by Nascimento et al. (2015).

The Shoshonitic Suite includes pyroxene-biotite gabbro/diorites and quartz diorites, sometimes with amphibole, and U-Pb zircon ages varying from 599 to 579 Ma. In the Porphyritic high-K Calc-Alkaline Suite predominate biotite + amphibole

porphyritic granites (subordinate granodiorites and quartz monzonites) with U-Pb zircon ages between 591 and 544 Ma. The Equigranular high-K Calc-Alkaline Suite is represented mainly by biotite granites (sometimes granodiorites), fine/medium equigranular, leucocratic, colored light gray, and U-Pb zircon ages from 582 to 527 Ma (Nascimento et al. 2015 and references therein).

The main Cambrian magmatism in the region refers to the bodies and dikes of pegmatitic granites and granitic pegmatites, with columbite and monazite U-Pb ages varying from 528 to 509 Ma (Baumgartner et al. 2006). Besides being an important source of industrial minerals (e.g. muscovite, K-feldspar, kaolinite, and quartz), most of these pegmatites are enriched with rare elements.

According to Jardim de Sá (1994), at least three important deformation events are recorded in the DPS. According to this author, the first event marked by gneiss-migmatite bands restricted to the basement rocks could have occurred in the Paleoproterozoic, reaching the amphibolite facies. The second phase is characterized by compression shear zones of dextral kinematics and isoclinal folds, inverted and recumbent, which originated a low angle S_2 foliation associated with metamorphism of green shale to amphibolite facies. This second deformation phase would have occurred during the Brasiliano Cycle. Transcurrent (dextral and sinistral) and transtensional shear zones, as well as isoclinal folds, mark the third deformation phase in the Jardim de Sá (1994) model,

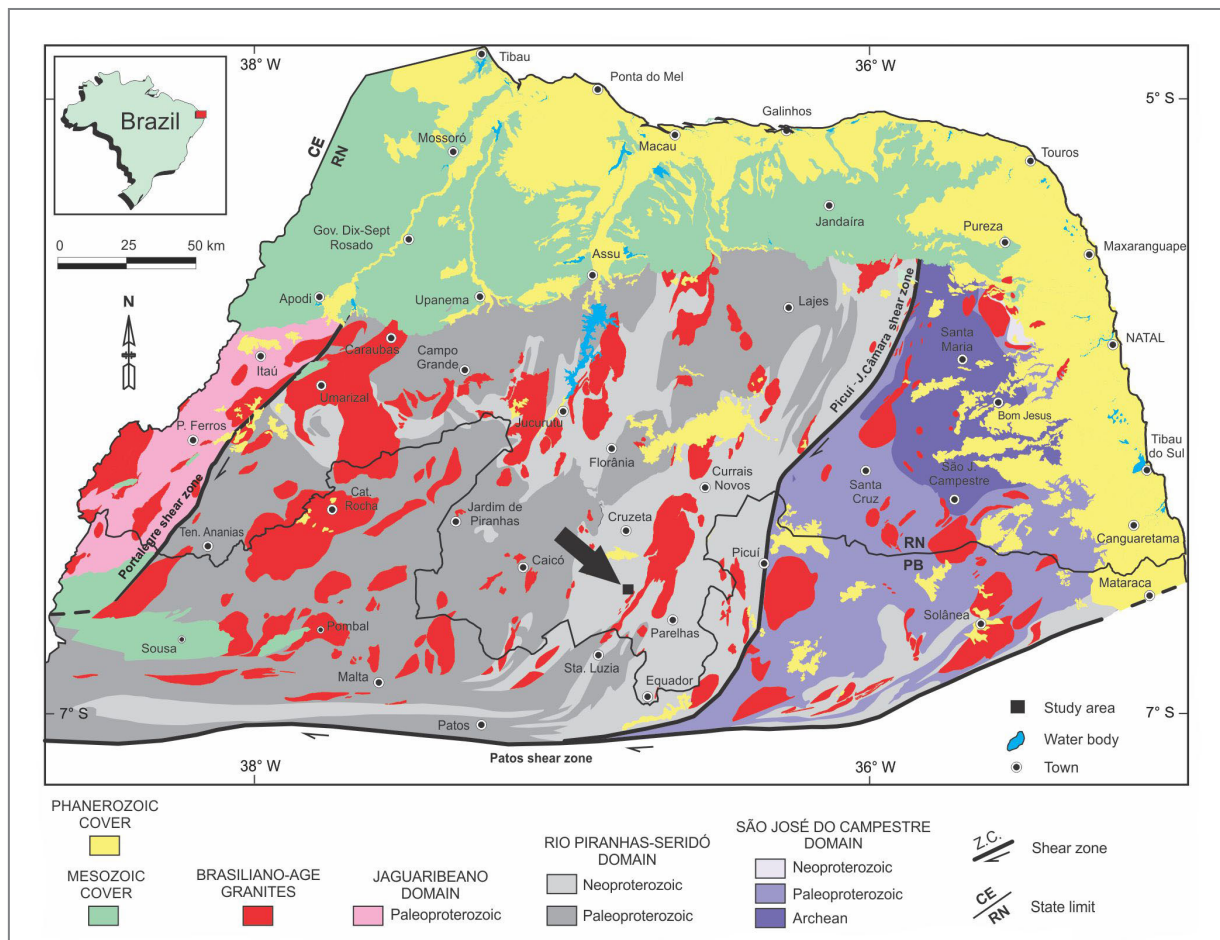


FIGURE 2 – Compartmentalization of the northeast portion of the Borborema Province, according to Medeiros et al. (2017), showing the study area (black arrow). RN = Rio Grande do Norte; PB = Paraíba; CE = Ceará.

TABLE 1 – Simplified stratigraphy for the Rio Piranhas-Seridó Domain according to Jardim de Sá and Salim (1980), Jardim de Sá (1984, 1994), Medeiros et al. (2017), Costa and Dantas (2014), and Costa et al. (2018).

Eon	Era	Period (age)	Lithostratigraphic Units
Phanerozoic	Paleozoic	Cambrian (485 - 541 Ma)	Pegmatitic bodies and dikes
Proterozoic	Neoproterozoic	Ediacaran (541 - ~635 Ma)	Equigranular High-K Calc-Alkaline Suite
			Porphyritic High K Calc-Alkaline Suite
			Shoshonitic Suite
			Seridó Group <table border="1" style="margin-left: 20px;"> <tr> <td>Seridó Formation</td> </tr> <tr> <td>Equador Formation</td> </tr> <tr> <td>Jucurutu Formation</td> </tr> </table>
Seridó Formation			
Equador Formation			
Jucurutu Formation			
Paleoproterozoic	Rhyacian (2050 - 2300 Ma)	Caicó Complex and augen gneisses	
		Siderian (2300 - 2500 Ma)	Árãbia Complex
Archean	Paleoarchean	- (3200 - 3600 Ma)	Amarante Complex

which is more widespread and marked by the refolding of the structures generated in the second deformation phase. The interference generates a NE-NNE trending coaxial refolding pattern. The metamorphism from greenschist facies to amphibolite is similar to that of the second deformation phase.

2.2. Local Geology

In this work, we refer to the Jardim do Seridó Suite (GJS), according to Cabral Neto et al. (2018), as consisting of a semicircular granitic stock with about 2 km² (GJS), associated with other smaller bodies and dikes that crop out 1 km south of Jardim do Seridó town, being intrusive in the garnet-biotite schists of the Seridó Formation (Figure 3).

These porphyro-lepidoblastic shales (garnet porphyroblasts varying from millimetric to 1.0 cm, Figure 4) are grayish colored with medium grain while some portions have a higher amount of quartz and plagioclase, providing a gneissic aspect to the rock. Its essential minerals are quartz (20-50%), plagioclase (5-20%), biotite (15-35%), and garnet (5-8%). Opaque minerals, zircon, apatite, tourmaline, muscovite and chlorite occur as accessories/traces (<3%). Quartz crystals are xenomorphic, elongated, oriented, and commonly exhibit undulating extinction. The oligoclase-type plagioclase occurs as xenomorphic crystals, oriented and altered to sericite sometimes. The oriented biotite crystals are lamellar, exhibiting brownish pleochroism and zircon and/or apatite inclusions. The octahedral garnet is hypidiomorphic to idiomorphic, showing atoll and poikiloblastic textures, with inclusions of quartz and opaque minerals. Its growth is late or postdates the main foliation (S_3). This foliation in the schists is quite evident and defined by the alignment of the biotite crystals and the stretching of the quartz crystals and venules. This structure is truncated by the bodies of the Jardim do Seridó Suite.

The Jardim do Seridó Suite generally crops out as large slabs (Figure 5A), dikes or blocks/boulders (Figure 5B). Two facies were identified here in the GJS. The main one consists of whitish leucocratic, medium-grained monzogranites,

bearing muscovite, garnet and biotite (Figure 6A). The rare opaque minerals observed are magnetite and chalcopyrite/pyrite.

Subordinate facies emerge in restricted areas, mainly at the edges of the main body (or near them, Figure 3) or as intrusive narrowbodies in the metapelites of the Seridó Formation, being represented by greyish biotite granodiorites, leucocratic, and fine-grained (Figure 6B).

Planar foliations lacking tectonic effects and indicative of magmatic flow (Figure 7), evidenced by the alignment of biotite crystals and feldspars, are features commonly observed in the main facies of the GJS.

In some outcrops, gradations were observed between the GJS medium grained facies and pegmatite portions (Figure 8A), as well as the capture of pegmatite phenocrysts by the GJS monzogranitic facies (Figure 8B).

Some field features evidence the intrusive relationship of the bodies of this suite in the metapelites of the Seridó Formation, such as: GJS dikes in the metapelites (Figure 5B) and the presence of garnet-biotite schist xenoliths (Seridó Formation) in GJS (Figure 9A) and partially assimilated, sometimes (Figure 9B).

The GJS intrusion relationship in the metapelites of the Seridó Formation is locally affected by pegmatite dikes that intrude both lithotypes (schists and granites), as highlighted in Figure 10.

3. Materials and methods

The lithochemical study was carried out from five analyses of the main facies (monzogranitic) of the GJS. The following methods were used: (i) X-ray fluorescence after dissolution with lithium metaborate or determining major elements and loss on ignition; (ii) ICP-MS after lithium metaborate fusion for determining trace and rare earth elements, and multi-acid digestion (HCl, HNO₃, HF and HClO₄) for trace elements; and (iii) specific ion for fluorine. The samples were prepared and analyzed in the SGS Geosol Laboratórios Ltda. Total iron is reported as Fe₂O₃.

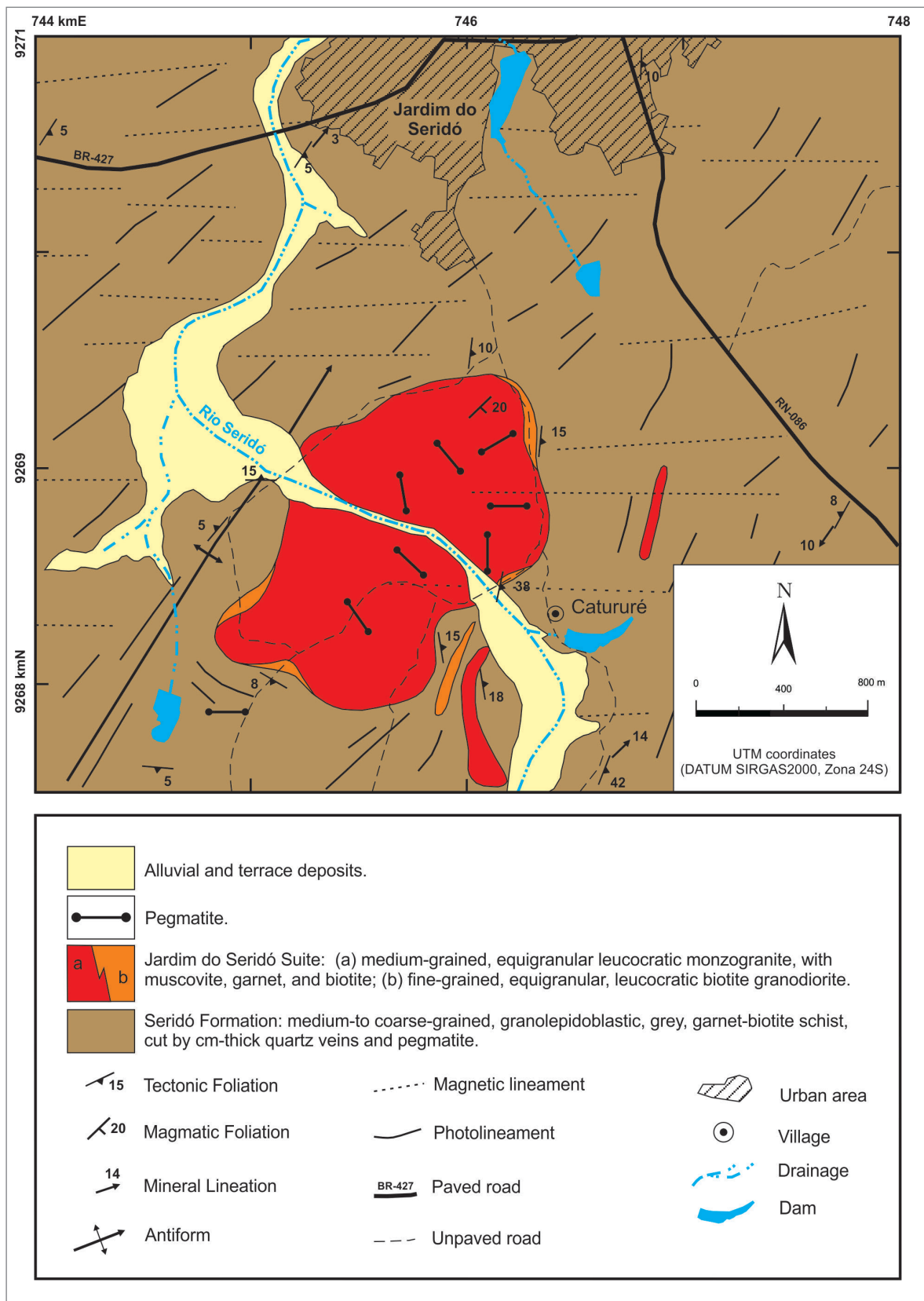


FIGURE 3 – Geological map of the southern area of the Jardim do Seridó town highlighting bodies of the Jardim do Seridó Suite.



FIGURE 4 – Plane view of the garnet-biotite porphyroblastic schist of the Seridó Formation, located 1.3 km south of Jardim do Seridó. Grt = garnet.

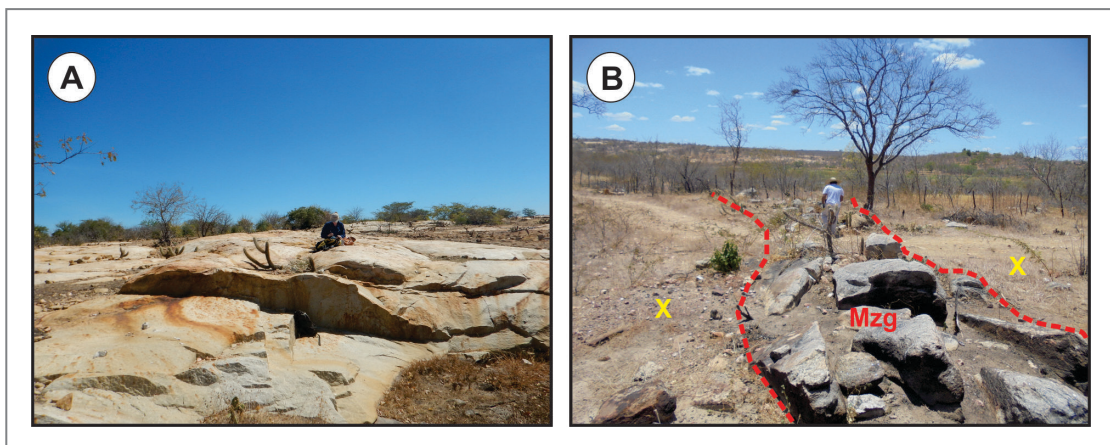


FIGURE 5 – A) Outcrop of the granitic stock of Jardim do Seridó. B) Monzogranite (Mzg) dike of the Jardim do Seridó intrusive in garnet-biotite schist (X) of the Seridó Formation. East portion of the stock.

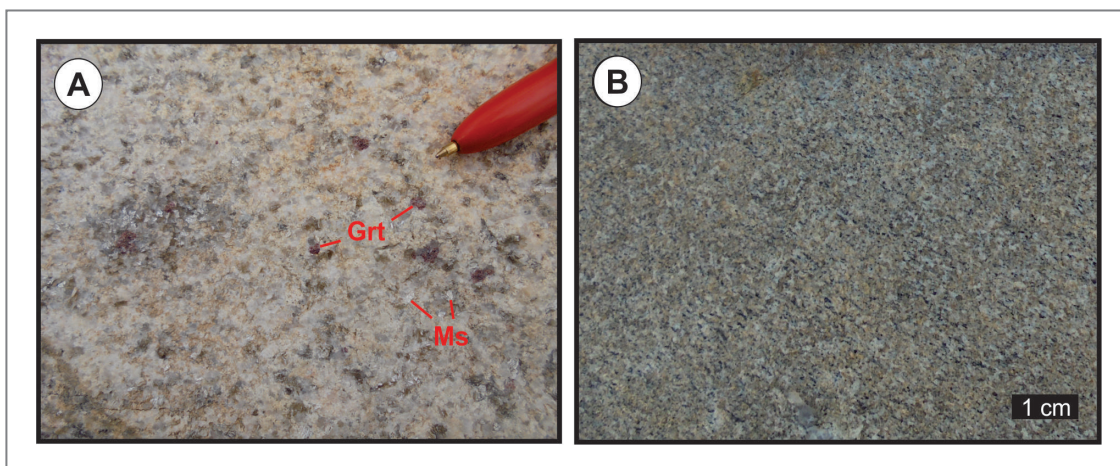


FIGURE 6 – A) Monzogranite with muscovite (Ms) and garnet (Grt), medium-grained, from the main facies of the Jardim do Seridó granitic stock. B) Leucocratic biotite granodiorite, fine-grained, from the eastern edge of the main body of the Jardim do Seridó Suite.

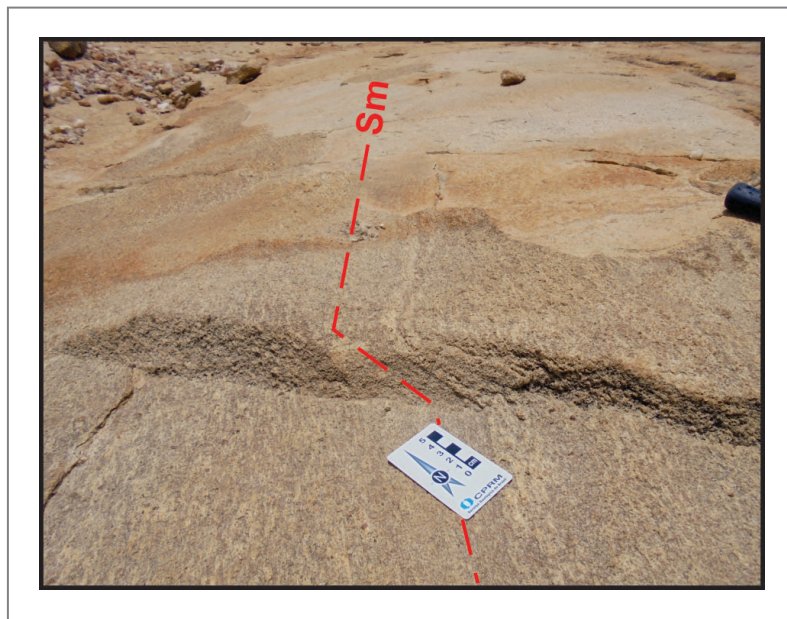


FIGURE 7 – Outcrop of monzogranite in the northern portion of the main body of the Jardim do Seridó Suite, showing a NE magmatic foliation (Sm).

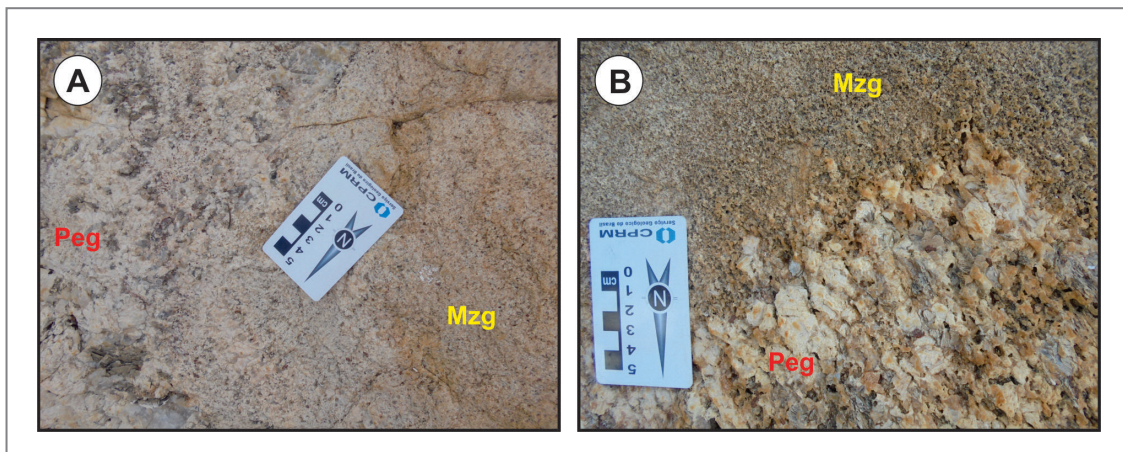


FIGURE 8 – A) Gradational contact between the monzogranite (Mzg) of the main facies of the Jardim do Seridó granitic stock and the pegmatitic portion (Peg). The northern portion of the body. B) Irregular contact between the monzogranite (Mzg) of the main facies of the Jardim do Seridó granitic stock and the pegmatitic portion (Peg), showing the capture of pegmatite phenocrysts by the monzogranite. The northern portion of the body.

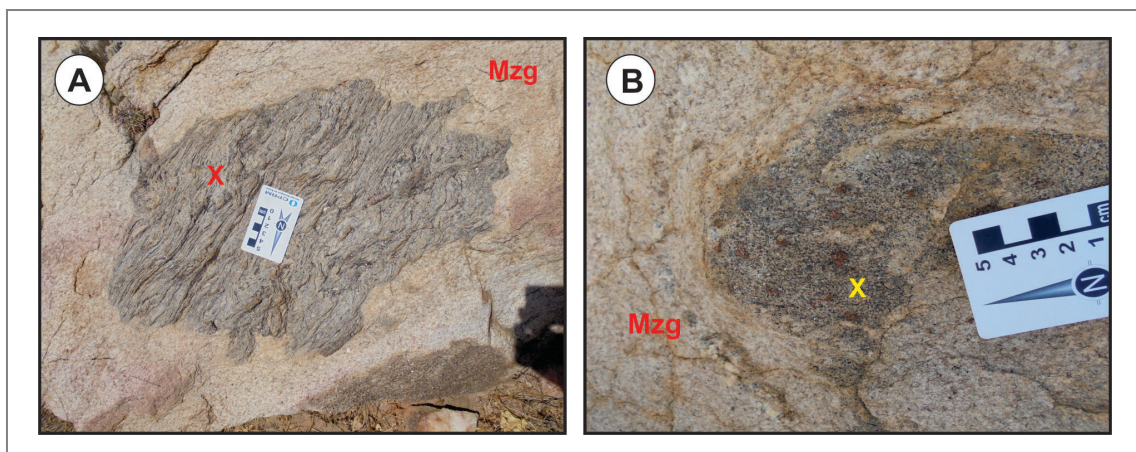


FIGURE 9 – A) Decimetric xenolith of biotite schist (X) from the Seridó Formation in the monzogranite (Mzg) of the Jardim do Seridó stock. Southeast portion of the body. B) Xenolith of the garnet-biotite schist of the Seridó Formation (X), partially assimilated, in the monzogranite (Mzg) of the Jardim do Seridó stock. The northern portion of the body.

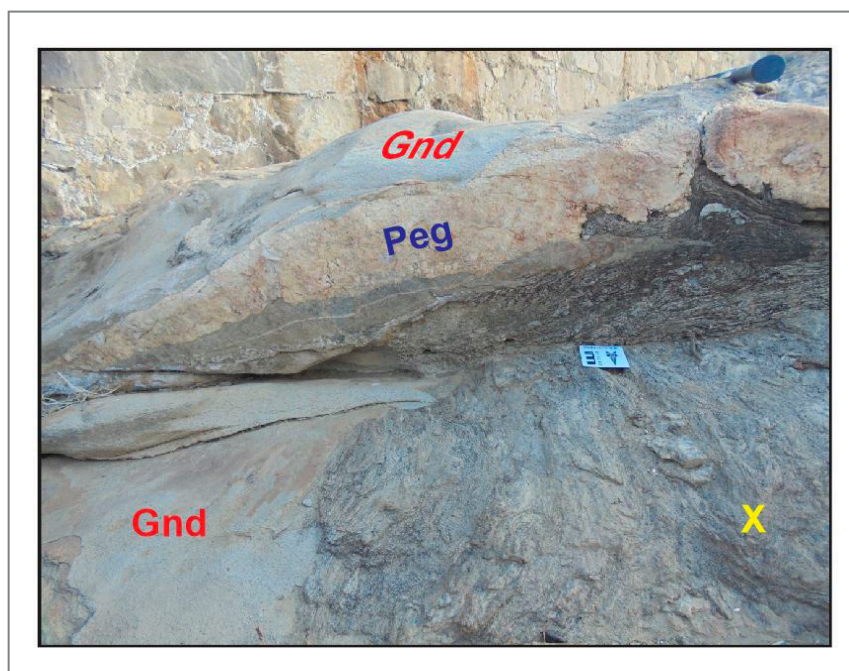


FIGURE 10 – Field relationship highlighting the intrusive contact of the GJS granodiorite (Gnd) in the schist biotite of the Seridó Formation (X), both later intruded by a pegmatitic dike (Peg).

A fresh and homogeneous sample of the monzogranitic facies was collected and used for the U-Pb zircon dating. The zircon crystals were prepared in the Grinding Laboratory of the Department of Geology of the Universidade Federal do Rio Grande do Norte, starting by crushing and wet sieving (500μ) the samples to separate and concentrate the heavy minerals (batting). After drying, the material went through the Frantz Magnetic Separator where the zircon grains were separated manually using a binocular loupe and analyzed in the Geochronology Laboratory of the Universidade de Brasília. The mounts were prepared, and the equipment used according to the methodology described by Cavalcante et al. (2018) and the procedures presented by Bühn et al. (2009). Further details on the adopted dating method can be obtained in Cavalcante et al. (2018). The ages were calculated and the corresponding graphs were plotted using the resources of the ISOPLOT 3.0 Ludwig (2003).

4. Results

4.1. Petrography

Two facies were identified in the GJS. The first one is the most expressive and is described in detail below. The second facies consists of greyish, leucocratic biotite-bearing granodiorite of equigranular and fine phaneritic texture. The essential minerals are plagioclase (40%), quartz (33%), K-feldspar (17%) and biotite (9%) whereas muscovite, opaque minerals, apatite, epidote, and zircon occur as accessories (1%). The feldspar crystals are commonly saussuritized.

The main facies consists of whitish monzogranites, equigranular to inequigranular, medium grained and leucocratic (5 to 9% of mafic minerals).

The essential minerals of this facies are microcline (31.0-41.0%), quartz (23.0-40.0%), plagioclase (22.0-30.0%), muscovite I (0.5-5.0%), garnet (0.5-5.0%), and biotite (0.5-

3.7%). As accessories (0.9%) occur opaque minerals, epidote I, allanite, zircon, apatite, titanite and, sometimes, rare amphibole crystals, while chlorite (0.5-1.0%), muscovite II and epidote II (0.1-0.2%) are observed as alteration minerals.

The microcline (0.4-5.0 mm) occurs as idiomorphic to subidiomorphic hypidiomorphic crystals, presenting a myrmekitic texture of the bulbous type at the plagioclase contact (Figure 11A), with inclusions of biotite, epidote I, zircon, apatite, quartz, muscovite I and opaque minerals. Muscovite II and saussurite crystals are the alteration products of this feldspar.

Quartz (0.1-2.4 mm) appears as xenomorphic to hypidiomorphic crystals with a commonly weak undulose extinction while elongated crystals with subgrains and recrystallized edges occur rarely. Quartz crystals can occur included in feldspars and garnet or having inclusions of zircon, biotite, apatite, opaque minerals and/or titanite.

Plagioclase (0.3-4.0 mm) of the oligoclase type (An_{23-25}) occurs as idiomorphic to hypidiomorphic crystals, having straight contacts with the microcline and biotite crystals. Inclusions of biotite, muscovite I, apatite, opaque minerals, zircon and/or titanite may be present whereas epidote II, muscovite II and calcite are the alteration products observed in this feldspar.

Muscovite I (0.3-3.5 mm) occurs as idiomorphic to hypidiomorphic crystals, elongated, lamellar, perfectly cleaved, situated in intergranular spaces (Figures 11B, C, D). It is observed dispersed and associated with biotite, in intergrowths with quartz (sharp and serrated contacts) and feldspar, which may contain zircon and/or quartz inclusions.

Garnet (1.0-5.0 mm) appears as idiomorphic to hypidiomorphic crystals, commonly with inclusions of quartz and feldspars (poikilitic texture), corroded edges, fractures and skeletal texture (Figure 11D) that may show contacts with quartz and feldspars varying from curved to straight.

The biotite (0.2-2.0 mm) is mostly present as idiomorphic to hypidiomorphic crystals with straight to serrated contacts

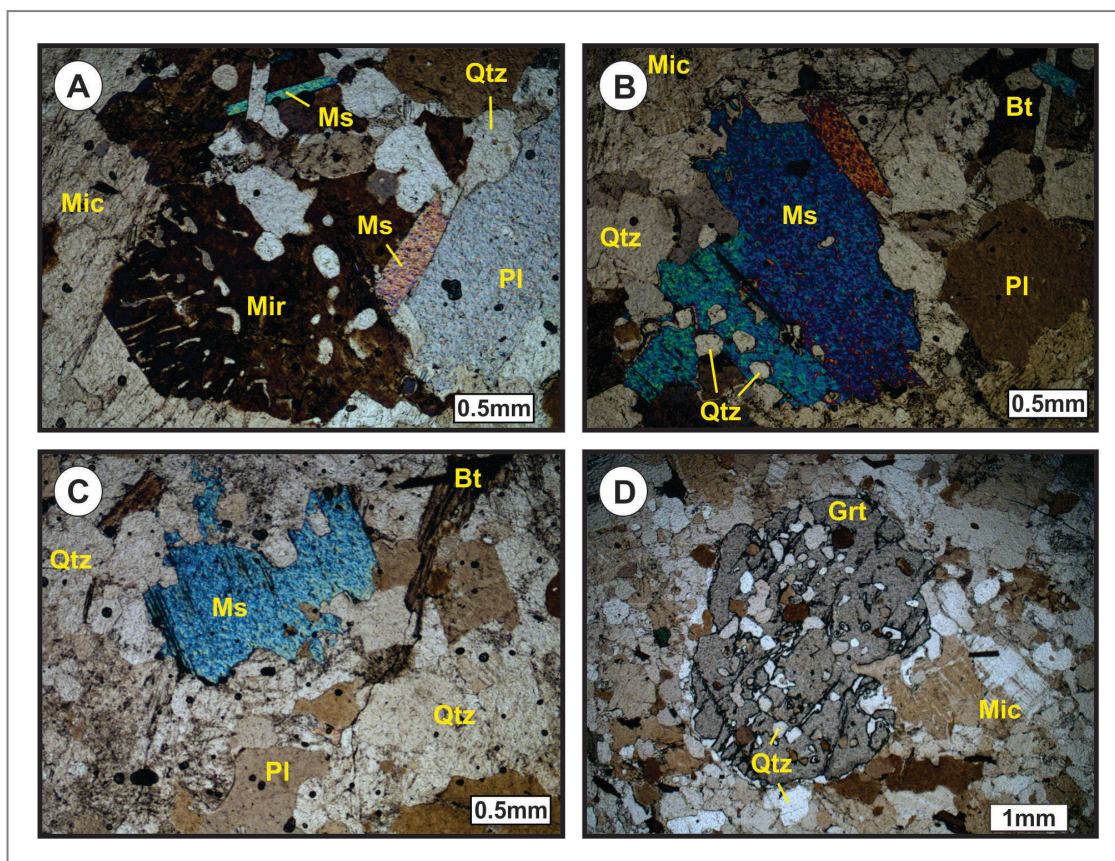


FIGURE 11 – Photomicrographs of the monzogranitic facies showing: A) Myrmekitic texture (Mir) of the bulbous type at the microcline (Mic) and plagioclase (Pl) contact. Ms-muscovite I; Qtz-quartz. Crossed Nicols. B) Elongated muscovite I (Ms) crystals with quartz inclusions (Qtz). Pl-Plagioclase; Mic-microcline; Bt-biotite. Crossed nicols. C) Association of muscovite I (Ms), plagioclase (Pl), microcline (Mic), biotite (Bt) and quartz (Qtz). Parallel nicols. D) Garnet crystal (Grt) with quartz inclusions (Qtz) and bordered by quartz matrix and microcline (Mic). Crossed Nicols.

with quartz and feldspar, where it is commonly included. It may contain inclusions of opaque minerals, zircon and/or apatite and sometimes occurs associated with chlorite, muscovite and allanite.

The titanite (0.5 mm) is hypidiomorphic, showing straight contacts with quartz and plagioclase, being included in these minerals. Epidote I (0.05-0.10 mm) is xenomorphic to hypidiomorphic, occurs included in quartz, feldspars, and biotite and, sometimes, bordering allanite (crown texture). The allanite is mostly hypidiomorphic, with crystals smaller than 0.1 mm and crowned by epidotes. Opaque minerals (0.1-0.2 mm) are crystalline to xenomorphic crystals appearing in quadratic or elongated sections, occurring dispersed in the matrix and rarely associated with biotite. They appear included in quartz, feldspar, and biotite. Apatite (0.1 mm) occurs as ovoid or prismatic crystals included in quartz, feldspars, and biotite. Zircon (<0.25 mm) occurs as idiomorphic to hypidiomorphic crystals, prismatic, sometimes zoned and rounded, and included in quartz, feldspar, biotite, and muscovite I.

The secondary minerals (0.1-0.4 mm) are usually xenomorphic to hypidiomorphic and represented mainly by muscovite II, epidote II and chlorite, of which the first two are associated with the alteration of plagioclase and the third, of biotite.

The crystallization of the magma for this facies (Figure 12) began with the formation of crystals of zircon, apatite and opaque minerals, while allanite, epidote I and titanite, are probably also of this phase, followed by the crystallization of

biotite and muscovite I. In the sequence, feldspars and quartz were formed, followed by garnet. Epidote II, calcite, muscovite II, chlorite, and myrmekite represent the subsolidus phase.

4.1.1. Crystallization conditions

The crystallization conditions were estimated based on the crystallization pressure, *liquidus* and *solidus* temperatures and oxygen fugacity (f_{O_2}) from the CIPW normative data and total rock analysis of SiO_2 and P_2O_5 .

The titanite + magnetite + quartz paragenesis, observed in thin section, indicates moderate to high f_{O_2} conditions above the FMQ buffer, according to Wones (1989). The late-magmatic processes are marked mainly by volatile-rich fluids (CO_2 , H_2O , and O_2), denoted by the carbonatization of plagioclase, myrmekitic texture, chloritization of biotite and saussuritization of plagioclase.

The pressures estimated based on the normative diagram of Tuttle and Bowen (1958) vary from 2 to 5 kbar (Figure 13). When plotted in the Harrison and Watson (1984) diagram, most samples occupy a field near the 800°C isotherm and only one sample plots in the vicinity of the 950°C isotherm. Early crystallization of apatite indicates that such temperatures are close to the *liquidus* (Figure 14A). The temperature estimated based on the normative diagram of Luth et al. (1964) shows values between 690-710°C, attributed to the *solidus* temperature (Figure 14B).

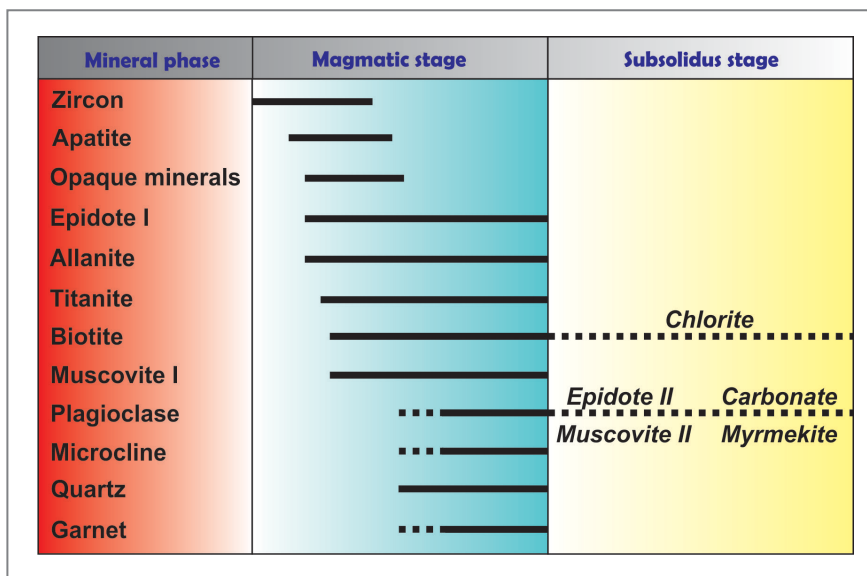


FIGURE 12 – Crystallization sequence established for the main facies (monzogranites) of Jardim do Seridó Suite.

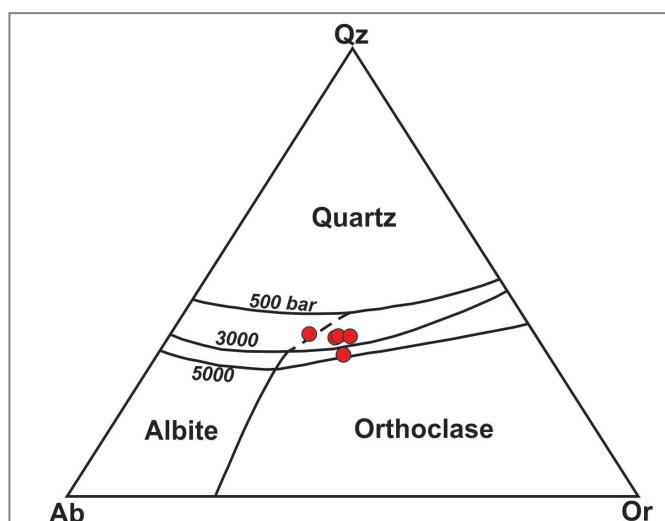


FIGURE 13 – Pressure estimates for the monzogranitic facies samples based on the normative diagram of Tuttle and Bowen (1958).

4.2. Whole Rock Geochemistry

The analyzed GJS samples (Table 2) show SiO₂ ranging between 74.3 - 77.0% and K₂O 5.1 - 3.9%, corroborating the high modal contents of the felsic paragenesis, and Al₂O₃ values ranging from 13.5-14.4%. In general, they are depleted in Na₂O (3.6-4.4%), Fe₂O₃ (1.3-1.6%), CaO (0.8-1.1%), TiO₂ (0.05-0.10%) and MgO (≤ 0.1%), due to their low contents of mafic minerals (M ≤ 8.3%).

Despite the narrow variation range of SiO₂ values and the small number of analyses, the results suggest possible correlations, positive for silica with Na₂O, Rb and Y; and negative for silica with Al₂O₃, Fe₂O₃, TiO₂, K₂O, Sr, Ba, Th, Nb, and Zr (Figures not included).

Using the alumina saturation index, the samples plotted in the weakly peraluminous field (Figure 15A and 15B), consistent with Sylvester (1989) classification, showing affinity with strongly fractionated alkali-to-alkali granitic rocks (Figure 16). However, the samples are predominantly calc-alkaline using the classification of Frost et al. (2001), (Figure 15B).

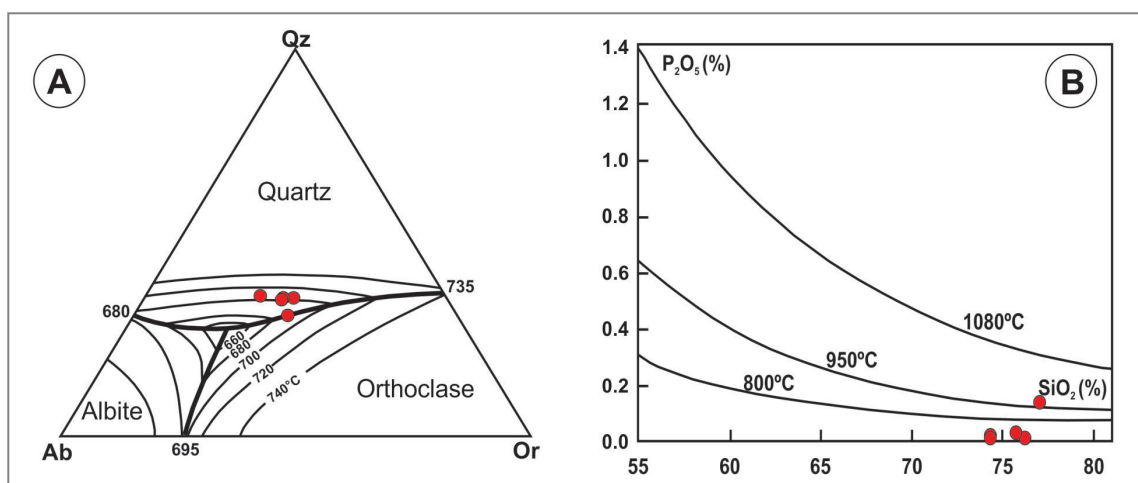


FIGURE 14 – A) Estimated crystallization temperature of apatite of the monzogranitic facies based on the Harrison and Watson diagram (1984). B) The estimated crystallization temperature of the monzogranitic facies based on the Qz-Ab-Or normative diagram of Luth et al. (1964) at 5 kbar P(H₂O).

TABLE 2 – Chemical analyses for major, minor and trace elements (including rare earth elements) of the monzogranitic facies of the Jardim do Seridó stock.

Element	FFU053	FFU054	FFU055	FFU421	FFU424
SiO ₂ (wt.%)	74.30	74.30	76.20	77.00	75.70
Al ₂ O ₃	13.50	14.40	13.80	13.60	13.50
Fe ₂ O ₃ t	1.60	1.38	1.44	1.33	1.40
MnO	0.05	0.03	0.05	0.09	0.04
MgO	<0.10	<0.10	<0.10	<0.10	<0.10
CaO	0.98	1.05	0.90	0.95	0.84
Na ₂ O	3.56	3.88	3.88	4.43	3.89
K ₂ O	4.86	5.14	4.72	3.87	4.60
TiO ₂	0.09	0.08	0.06	0.05	0.06
P ₂ O ₅	0.01	0.02	<0.01	0.14	0.03
PF	0.18	0.39	0.26	0.15	0.23
Total	99.13	100.67	101.31	101.61	100.29
Rb (ppm)	248.60	279.90	356.20	337.20	312.80
Ba	378.00	237.00	171.00	146.00	193.00
Sr	83.80	67.20	56.20	44.60	57.10
Zr	75.80	85.10	65.50	52.10	63.40
Ni	1.00	1.20	0.50	1.70	2.20
V	5.00	5.00	3.00	5.00	5.00
Nb	26.60	57.60	31.90	28.80	33.60
Y	14.20	15.30	21.70	26.56	34.93
Li	77.00	89.00	89.00	84.00	103.00
Cu	4.60	16.60	4.10	31.20	1.30
Pb	42.90	56.20	50.40	22.20	33.60
Zn	32.00	23.00	25.00	27.00	15.00
W	1.90	4.50	1.20	0.80	0.90
Mo	0.77	0.92	8.10	1.86	1.01
Ta	2.71	16.27	3.24	7.95	6.33
Nb	26.60	57.60	31.90	28.80	33.60
Th	30.70	32.30	26.60	17.60	21.70
U	11.78	16.29	15.55	13.67	13.47
Hf	2.32	1.95	2.26	1.81	2.49
Na ₂ O+K ₂ O	8.42	9.02	8.60	8.30	8.49
Na ₂ O/K ₂ O	0.73	0.75	0.82	1.14	0.85
A/CNK	1.05	1.04	1.05	1.03	1.04
A/NK	1.21	1.20	1.20	1.18	1.19
La (ppm)	29.70	22.50	14.20	12.60	20.50
Ce	54.48	43.09	27.32	9.71	16.27
Pr	5.22	4.45	3.24	1.89	3.58
Nd	18.60	16.70	11.60	6.80	13.20
Sm	3.80	4.40	3.10	1.90	3.10
Eu	0.51	0.46	0.36	0.25	0.42
Gd	3.96	5.38	3.98	2.46	3.51
Tb	0.66	1.14	0.73	0.50	0.67
Dy	4.23	7.79	5.37	3.84	4.60
Ho	0.90	1.76	1.26	0.86	1.03
Er	2.78	5.48	4.23	2.71	3.53
Tm	0.48	0.86	0.67	0.45	0.52
Yb	3.10	6.70	5.30	3.60	4.20
Lu	0.51	1.05	0.91	0.14	0.26
(La/Yb) _N	6.47	2.27	1.81	2.36	3.29
(La/Sm) _N	4.92	3.22	2.88	4.18	4.16
(Gd/Yb) _N	1.03	0.65	0.61	0.55	0.68
Eu/Eu*	0.40	0.29	0.31	0.35	0.39

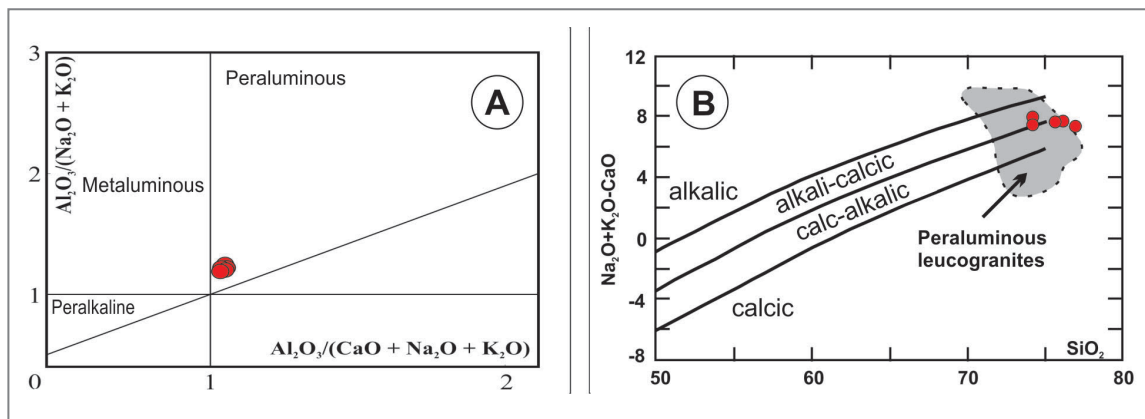


FIGURE 15 – A) Shand diagram plotting the aluminum saturation index (fields according to Maniar and Piccoli 1989) for the monzogranitic facies. B) Alkalis vs. silica diagram with the gray polygon representing the composition range of the peraluminous leucogranites (Frost et al. 2001), including the monzogranitic facies samples (red circles).

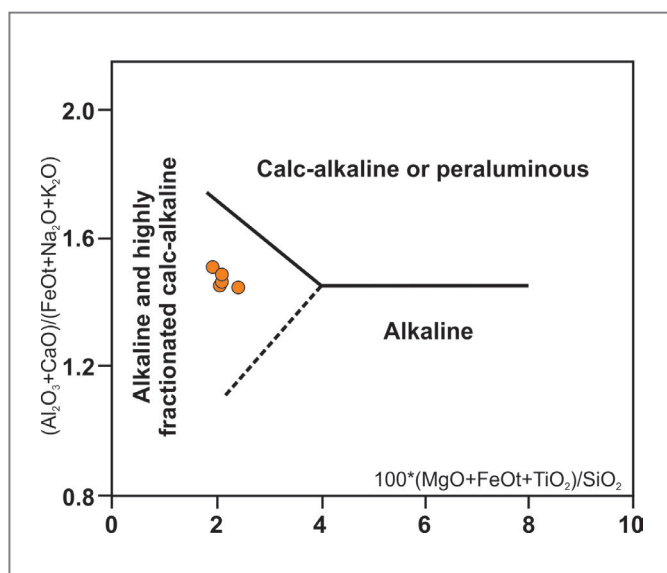


FIGURE 16 – Sylvester (1989) discriminant diagram for the monzogranitic facies of the Jardim do Seridó Suite.

The analytical data on rare earth elements (REE, Table 2) were normalized for chondrite according to Evensen et al. (1978). The summation values oscillate between 47.71-128.93 ppm, averaging about 91.21 ppm, probably indicating an impoverishment trend of the total REE content from the increasing SiO_2 content (Table 2). In general, the fractionation pattern has negative slope between La and Lu ($La/Yb)_N = 1.81-6.47$, where the light rare earth elements (LREE) display a fractionated and slightly convex characteristic ($La/Sm)_N = 2.88-4.92$, but the heavy rare earth elements (HREE) have sub-horizontal and smooth concave distribution ($Gd/Yb)_N = 0.55-1.03$. The lower Ce and Lu values observed in two samples (Figure 17) can be attributed to the probable incipient alteration processes associated with the microfractures observed in thin section.

The Eu/Eu^* ratios vary from 0.29 to 0.40, revealing pronounced negative anomalies that may be related to the greater plagioclase fractionation during the magma evolution that generated the rocks of this granite stock or the partial melting of continental crustal sources at low pressures.

The GJS samples were plotted in discriminant diagrams of tectonic environment. In the discriminant diagrams of Pearce et al. (1984) and Thiéblemont and Cabanis (1990), the granites show affinities with rocks from syn-collisional environments (Figures 18, 19).

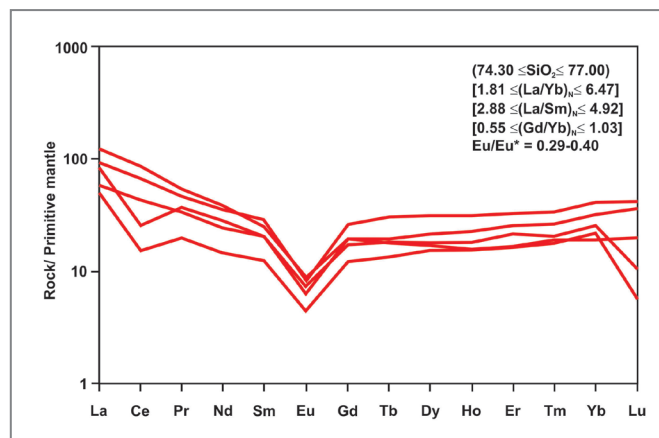


FIGURE 17 – REE diagram for the monzogranitic facies with normalizing factors according to Evensen et al. (1978).

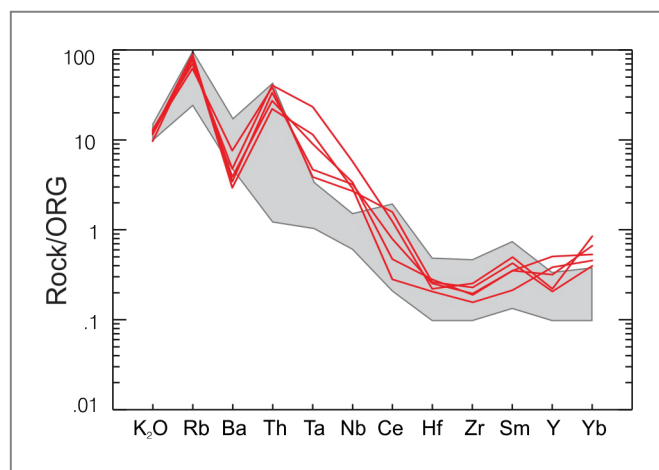


FIGURE 18 – Multi-element diagram for tectonic setting normalized by ORG with syn-collisional rocks (gray polygon), according to Pearce et al. (1984), and the monzogranitic facies samples (red lines).

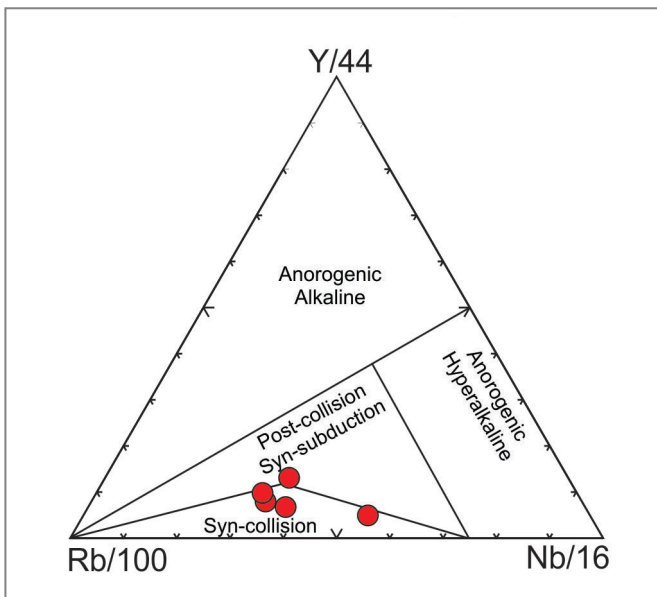


FIGURE 19 – Thiéblemont and Cabanis (1990) diagram of tectonic setting with monzogranitic facies samples.

4.3. U-Pb zircon dating

A monzogranite sample containing biotite, muscovite and garnet was collected from the outcrop FV-125 for U-Pb zircon dating (Figure 20). The analyzed zircon crystals are generally clear, free of fractures or rims intergrowth, prismatic and elongated, about 150-200 μm long (length/width = 2.5 to 4.5). They are euhedral and usually present zoning parallel to the crystal faces (igneous). Some crystals, however, present

small (10-20 μm) circular or ovoid inclusions (among them monazite), fractures and areas with dark spots (percolation of fluids). For more precise results, the analyses were preferably performed in clean areas, without inclusions (Figure 21A). Despite this, the data of nine crystals were discarded due to high analytical error (1sigma) or common lead content (both greater than > 3%).

This cut-off criterion allowed the data of 26 crystals that are distributed in two populations. The first group is very discordant and dispersed (Table 3, crystals 4, 6, 14, 18, 19, 23, 26, 29, 2, 30 and 33), a dispersion that may have been caused by mixing the zircon composition with not observed inclusions (submicroscopic and/or in depth). The other group is more concordant and presents $^{206}\text{Pb}/^{238}\text{U}$ apparent ages between 577 and 625 Ma, which were calculated using a coherent group of points for which the $^{206}\text{Pb}/^{238}\text{U}$ and $^{207}\text{Pb}/^{235}\text{U}$ age discordance are lower than 1%. This filter allowed five data (crystals 10, 17, 20, 24, 25) that indicated the concordia age of 592 ± 2 Ma (Figure 21B), associated with MSWD of 2.8, interpreted as the best estimate for the crystallization age of the monzogranite of the Jardim do Seridó stock.

5. Discussion about the GJS fertility

Selway et al. (2005) define fertile granite as a parental granite of pegmatite dikes mineralized to rare elements commonly presenting: (i) high silica content (> 69% SiO_2); (ii) $\text{Al}_2\text{O}_3/\text{CaO} + \text{Na}_2\text{O} + \text{K}_2\text{O}$ ratio > 1 (peraluminous); (iii) muscovite, garnet, tourmaline, apatite, cordierite, andalusite and/or topaz; (iv) low Fe, Mg and Ca contents; (v) enrichment in rare elements (Li, Ta, Cs, Ga, Nb, Rb and/or Sn), generally greater than three times the average value of the upper continental crust (Table 4); (vi) K/Rb and K/Cs ratios lower

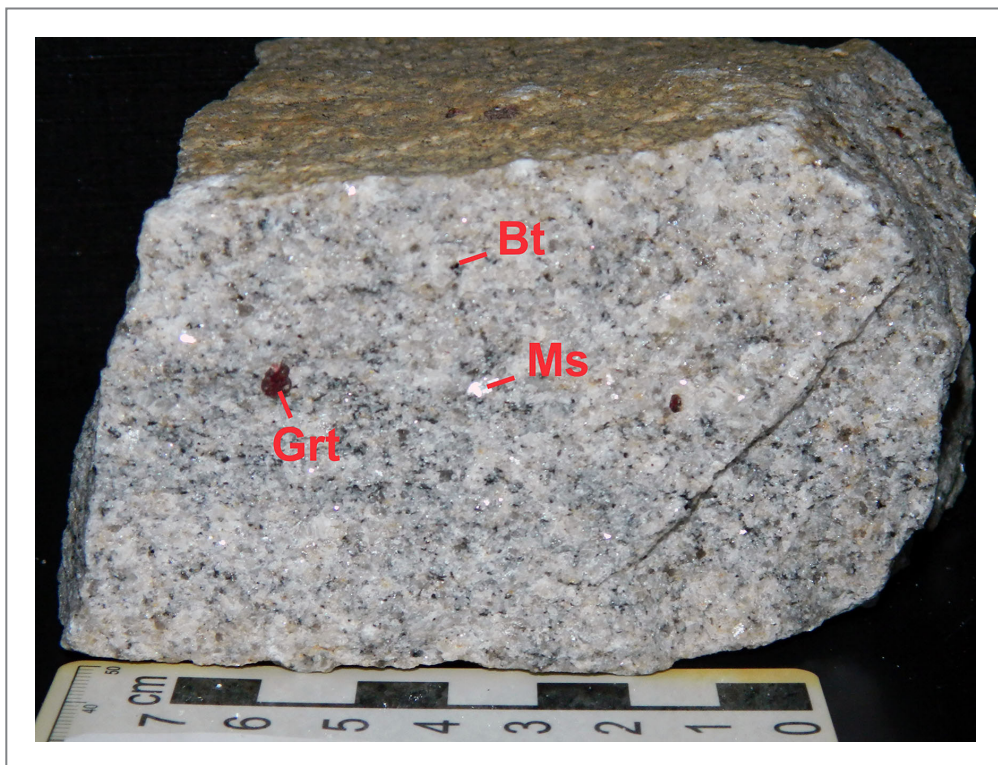


FIGURE 20 - Photograph of the dated monzogranite sample from the stock of the Jardim do Seridó Suite. Bt = biotite; Ms = muscovite; Grt = garnet.

TABLE 3 – U-Pb isotopic data of zircon crystals of the monzogranite in Jardim do Seridó (FV-125). UTM coordinates: 746,157 mE; 9,268,748 mN (Zone 24S, SIRGAS2000).

Spot grain	f206 (%)	Th/U	Pb ²⁰⁶ /Pb ²⁰⁴	Pb ²⁰⁷ /Pb ²⁰⁶	err (%) 1σ.	Pb ²⁰⁷ /U ²³⁵	err (%) 1σ.	Pb ²⁰⁶ /U ²³⁸	err (%) 1σ.	Rho	Pb ²⁰⁷ /Pb ²⁰⁶ (Ma)	Pb ²⁰⁶ /U ²³⁸ (Ma)	Pb ²⁰⁷ /U ²³⁵ (Ma)	Conc.(%)
012-ZR10*	0.28	0.597	5498	0.05997	0.89	0.798	1.20	0.0965	0.72	0.60	602 ± 38	594 ± 8	596 ± 11	99.70
022-ZR17*	0.13	0.806	11985	0.06033	0.47	0.804	0.92	0.0967	0.70	0.76	615 ± 20	595 ± 8	599 ± 8	99.28
027-ZR20*	0.19	0.760	8406	0.05952	0.67	0.780	1.05	0.0950	0.71	0.68	586 ± 29	585 ± 8	585 ± 9	99.95
031-ZR24*	0.05	0.852	32055	0.05974	0.47	0.785	0.88	0.0953	0.64	0.73	594 ± 20	587 ± 7	588 ± 8	99.73
032-ZR25*	0.21	0.971	7269	0.06054	0.72	0.806	0.94	0.0966	0.47	0.50	623 ± 31	594 ± 5	600 ± 8	99.00
003-ZR01	0.21	0.636	7463	0.05831	0.70	0.767	0.97	0.0954	0.56	0.58	541 ± 30	588 ± 6	578 ± 9	101.62
005-ZR03	0.23	0.538	6815	0.06011	0.47	0.812	0.87	0.0980	0.63	0.72	608 ± 20	603 ± 7	604 ± 8	99.82
010-ZR08	0.25	0.753	6208	0.05852	0.67	0.765	1.08	0.0948	0.76	0.70	549 ± 29	584 ± 8	577 ± 9	101.20
034-ZR27	0.08	0.519	18805	0.05857	0.75	0.778	0.99	0.0964	0.52	0.53	551 ± 33	593 ± 6	584 ± 9	101.46
004-ZR02	0.51	0.856	3043	0.06154	0.72	0.794	1.06	0.0936	0.69	0.65	658 ± 31	577 ± 8	594 ± 10	97.17
020-ZR15	0.05	0.890	34302	0.05945	0.39	0.801	0.72	0.0977	0.47	0.66	584 ± 17	601 ± 5	597 ± 6	100.59
021-ZR16	0.06	0.853	26647	0.05974	0.42	0.838	0.86	0.1018	0.65	0.76	594 ± 18	625 ± 8	618 ± 8	101.06
028-ZR21	0.08	0.529	19454	0.05945	0.49	0.805	1.02	0.0982	0.82	0.80	584 ± 21	604 ± 9	600 ± 9	100.71
036-ZR29-1	0.12	0.013	13402	0.05966	0.65	0.817	1.04	0.0993	0.73	0.70	591 ± 28	610 ± 8	606 ± 10	100.65
039-ZR29-2	0.15	0.699	10440	0.06157	0.74	0.731	1.95	0.0861	1.76	0.91	659 ± 31	533 ± 18	557 ± 17	95.57
041-ZR31	0.35	0.160	4462	0.06168	0.99	0.819	1.22	0.0963	0.60	0.49	663 ± 42	593 ± 7	608 ± 11	97.56
024-ZR19	1.07	1.011	1454	0.06722	2.22	0.940	2.40	0.1014	0.83	0.34	845 ± 91	623 ± 10	673 ± 23	92.50
006-ZR04	1.18	0.786	1316	0.07015	1.84	0.985	1.96	0.1018	0.55	0.28	933 ± 75	625 ± 7	696 ± 20	89.78
019-ZR14	0.67	0.035	2322	0.07183	0.88	0.891	1.10	0.0900	0.54	0.49	981 ± 36	555 ± 6	647 ± 10	85.84
033-ZR26	0.89	0.208	1760	0.07286	1.76	0.819	2.48	0.0815	1.70	0.69	1010 ± 71	505 ± 17	607 ± 23	83.16
029-ZR22	1.11	0.836	1407	0.07495	3.03	0.990	3.12	0.0958	0.63	0.20	1067 ± 119	590 ± 7	699 ± 31	84.40
043-ZR33	2.11	0.604	738	0.07499	0.81	0.937	1.07	0.0906	0.60	0.56	1068 ± 32	559 ± 6	671 ± 11	83.29
023-ZR18	1.05	0.686	1481	0.07848	0.72	0.978	1.10	0.0904	0.74	0.67	1159 ± 28	558 ± 8	692 ± 11	80.53
008-ZR06	2.80	0.371	555	0.08500	0.90	1.076	1.08	0.0918	0.48	0.44	1316 ± 35	566 ± 5	741 ± 11	76.33
030-ZR23	2.90	0.659	538	0.08643	1.26	1.056	1.69	0.0886	1.07	0.63	1348 ± 48	547 ± 11	732 ± 18	74.78
040-ZR30	0.10	0.738	16218	0.09084	2.39	1.217	2.69	0.0972	1.18	0.44	1443 ± 90	598 ± 13	808 ± 30	73.94

*Analyses used for age calculation

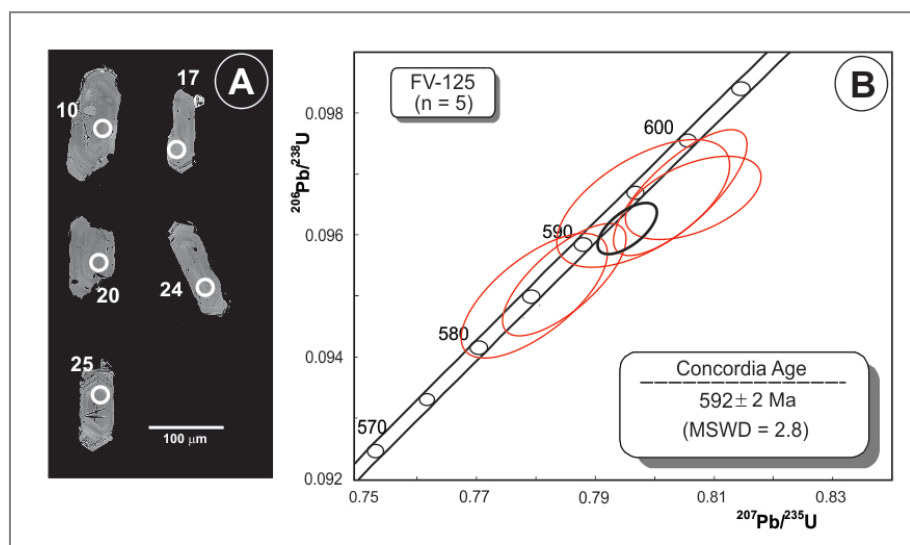


FIGURE 21 – A) Backscattered electron images of the zircon crystals used to calculate the age of the Jardim do Seridó monzogranite (sample FV-125). Numbers identify the analysis. B) Concordia diagram (U-Pb zircon) for the Jardim do Seridó monzogranite (sample FV-125).

than the mean of the upper continental crust (K/Rb = 252 and K/Cs = 7630, according to Taylor and McLennan 1985); (vii) Mg/Li <10, and (viii) Nb/Ta <8.

As shown previously, the GJS monzogranites are evolved (74.3-77.0% SiO₂), peraluminous (Al₂O₃/CaO + Na₂O + K₂O > 1), predominantly potassic (0.9 <K₂O/Na₂O <1.4), with muscovite and garnet in their modal composition and low Fe (1.33-1.60% Fe₂O₃t), Mg (MgO <0.1%) and Ca (0.84-1.05% CaO) contents.

Additionally, these rocks are enriched in Be, Li, Nb, Rb, and Ta, with values greater than three times the average upper continental crust and comparable to those of fertile leucogranites (Table 4). The Nb and Ta levels in these monzogranites are, in general, substantially higher than in fertile leucogranites.

Cerný and Meintzer (1988) and Cerný (1989), based on chemical analyses of total rock of granites, used elemental ratios to characterize the fertile suite. Table 5 presents the GJS values for some of these ratios.

The K/Rb and K/Cs ratios in the GJS monzogranite vary respectively from 91 to 121 and from 2550 to 6250 (Table 5),

TABLE 4 – Abundance of some rare elements in the upper continental crust (mean values), fertile leucogranites and monzogranites of the Jardim do Seridó stock. Values expressed as ppm. Data source: ¹Taylor and McLennan (1985) and ²Cerný and Meintzer (1988).

Element	Crust ¹	Fertile leucogranite ²	Monzogranites of the Jardim do Seridó Suite
Be	3	<0.5-61	7.6-18.2
Cs	3.7	<0.5-39	4.27-9.73
Ga	17	<10-81	18.2-20.90
Li	20	1-1400	77-103
Nb	25	<1-81	76-164.57
Rb	112	33-1050	710.29-1017.71
Sn	5.5	<1-44	1.2-3.60
Ta	2.2	2-8.5	135.50-813.50

TABLE 5 – Element ratios obtained in whole-rock analyses of monzogranitic facies samples of the Jardim do Seridó stock

Sample	K/Rb	K/Cs	K/Ba	Rb/Sr	Mg/Li	Nb/Ta
FFU053	121	5017	80	3	12	12
FFU054	102	3167	120	4	8	5
FFU055	103	5243	215	7	4	12
FFU421	91	2550	403	15	2	4
FFU424	120	6250	310	8	2	8

being well below the mean values of the upper continental crust and within the range of fertile granites (Figures 22A, B). The K/Ba (80-403) and Rb/Sr (3-15) ratios (Table 5) are within the ranges of 48 -18,200 and 1.6-185 for fertile granites (Figures 22C, D), respectively, according to Cerný (1989). Four samples presented Mg/Li ratio values below 10 (Table 5), thus being within the range of 1.7-50 (Figure 22E) characteristic of fertile granites according to Cerný (1989). The Nb/Ta ratio of all analyzed samples are within the compositional range of fertile granites (0.1-12, according to Cerný and Meintzer 1988), three of them having values equal to or lower than 8 for this ratio (Table 5 and Figure 22F), indicating high fertility.

Peraluminous granitoids with similar ratios were characterized as fertile and possible source of pegmatites mineralized to rare elements in the Eastern Pegmatitic Province of Brazil (Médio Jequitinhonha region), in Minas Gerais (Paes et al. 2016).

6. Conclusions

Two facies were recognized in the GJS. The dominant facies consists of a whitish, leucocratic, medium-grained, phaneritic, equigranular to inequigranular monzogranite containing muscovite, garnet and biotite. The less expressive facies consists of a greyish-colored, fine-grained, phaneritic, equigranular biotite-bearing leucocratic granodiorite.

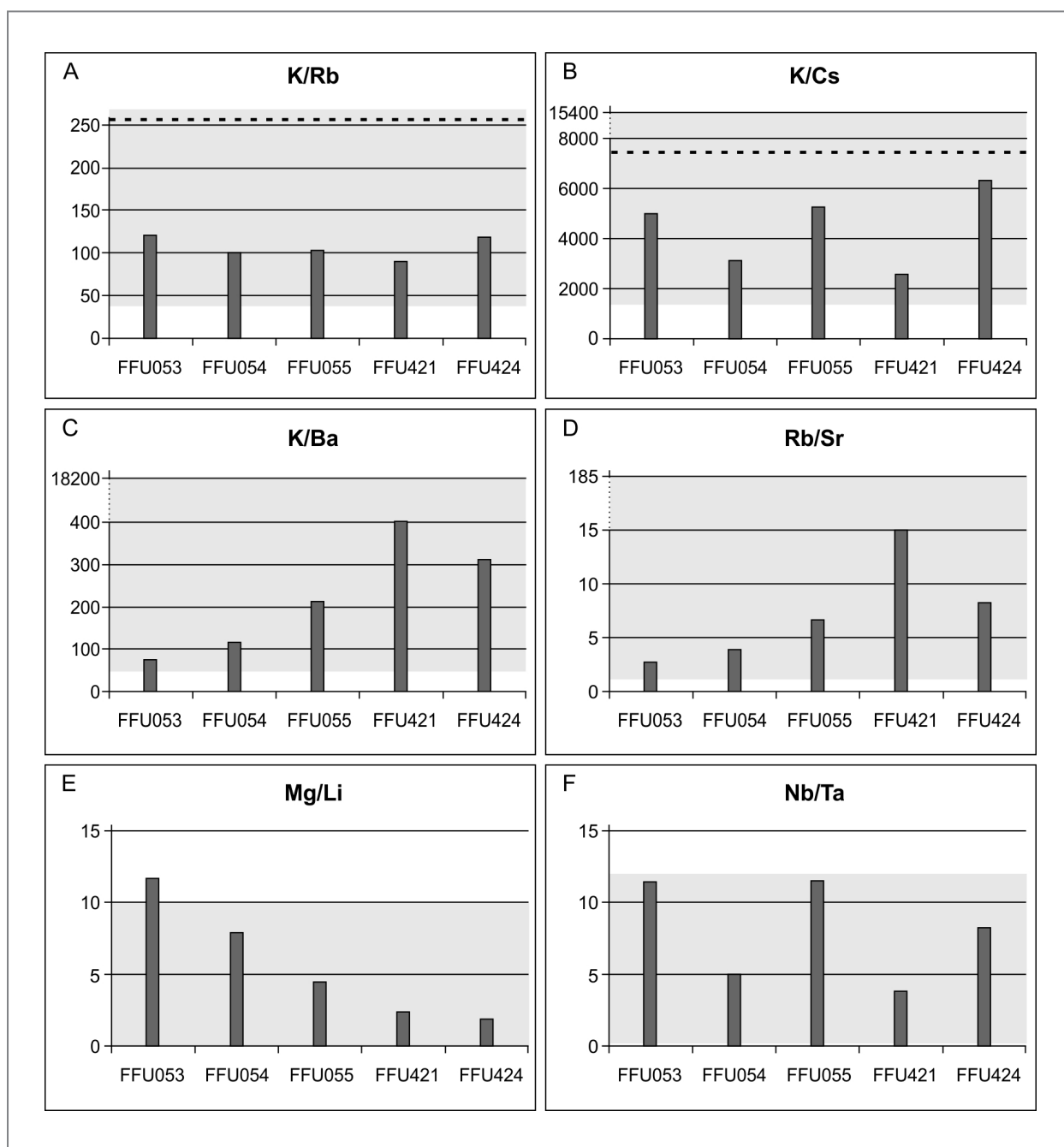


FIGURE 22 – Histograms showing the K/Rb (A), K/Cs (B), K/Ba (C), Rb/Sr (D), Mg/Li (E), and Nb/Ta (F) ratios of the monzogranitic facies samples, indicating the compositional interval of the fertile granites in light grey (Cerný and Meintzer 1988; Cerný 1989) and the mean values of the K/Rb and K/Cs ratios of the upper continental crust in dashed thick line, according to Taylor and McLennan (1985).

The estimated pressures for the monzogranite samples based on the normative quartz-albite-orthoclase composition vary from 2 to 5 kbar, while crystallization temperatures ranged from 690 (*solidus*) to 950°C (*liquidus*).

The monzogranite lithochemical data indicate that these rocks have a peraluminous signature, a fact that is corroborated by the muscovite and garnet paragenesis, while the tectonic setting diagrams suggest that these rocks are syn-collisional.

The 592 Ma age obtained for the GJS allowed to define an Ediacaran age and, consequently, to record the existence of a peraluminous suite associated with the Brasiliano Orogenesis in the Rio Piranhas-Seridó Domain of the Borborema Province.

Altogether the analysis of the GJS characteristics allows characterizing it as a fertile granite, i.e., a granite capable of generating pegmatites mineralized to rare elements.

Acknowledgments

The authors thank the CPRM-Geological Survey of Brazil, through the projects “Evaluation of Lithium Potential in Brazil: Borborema Province Pegmatitic Area” and “Crustal Evolution and Metallogeny of the Seridó Mineral Province”, for releasing the data presented here. Thanks are also due to the Department of Geology of the Universidade Federal do Rio Grande do Norte and the Laboratory of Stable Isotopes

of the Universidade de Brasília for their support in the sample preparation and the acquisition of analytical results, as well as to the reviewers for their suggestions, which greatly contributed to the improvement of this manuscript.

References

- Almeida F.F.M., Hasui Y., Brito Neves B.B. de, Fuck R.A. 1977. Províncias estruturais brasileiras. In: Simpósio de Geologia do Nordeste, 8, 363-391.
- Almeida F.F.M., Hasui Y., Brito Neves B.B. de, Fuck R.A. 1981. Brazilian structural provinces: an introduction. *Earth-Science Reviews*, 17, 1-29. [https://doi.org/10.1016/0012-8252\(81\)90003-9](https://doi.org/10.1016/0012-8252(81)90003-9)
- Angelim L.A.A., Nesi J.R., Torres H.H.R., Medeiros V.C., Santos C.A., Veiga Júnior J.P., Mendes V.A. 2006. Geologia e recursos minerais do estado do Rio Grande do Norte. Recife: CPRM, 119 p. Available on line at: <http://rigeo.cprm.gov.br/jspui/handle/doc/10234>
- Baumgartner R., Romer R.L., Moritz, R., Sallet R., Chiaradia M. 2006. Columbite-tantalite-bearing granitic pegmatites from the Seridó Belt, northeastern Brazil: genetic constraints from U–Pb dating and Pb isotopes. *The Canadian Mineralogist*, 44(1), 69-86. <https://doi.org/10.2113/gscanmin.44.1.69>
- Brito Neves B.B. de, Santos E.J., Van Schmus W.R. 2000. Tectonic history of the Borborema province, northeastern Brazil. In: International Geological Congress, 31, 151-182.
- Brito Neves B.B. de. 1975. Regionalização geotectônica do Pré-cambriano Nordestino. São Paulo. PhD Thesis, Universidade de São Paulo, São Paulo, 198 p. <https://doi.org/10.11606/T.44.1975.tde-21062013-104857>
- Brito Neves B.B. de. 1983. O mapa geológico do Nordeste Oriental do Brasil, escala 1:1.000.000. Thesis, Universidade de São Paulo, São Paulo, 177 p. <https://doi.org/10.11606/T.44.2013.tde-30102013-131731>
- Bühn B., Pimentel M.M., Matteini M., Dantas E.L. 2009. High spatial resolution analysis of Pb and U isotopes for geochronology by laser ablation multi-collector inductively coupled plasma mass spectrometry (LA-MC-IC-MS). *Anais da Academia Brasileira de Ciências*, 81(1), 99-114. <http://dx.doi.org/10.1590/S0001-37652009000100011>
- Cabral Neto I., Silveira F.V., Fernandes P.R., Paes V.J.C., Santos L.D., Medeiros V.C. 2018. Mapa geológico e de recursos minerais de lítio - Província Pegmatítica da Borborema, Escala 1:250.000. Programa Geologia, Mineração e Transformação Mineral, Natal, CPRM. Available on line at: <http://geosgb.cprm.gov.br/> (accessed on 26 December 2018).
- Caby R., Sial A.N., Arthaud M., Vauchez A. 1991. Crustal evolution and the Brasiliano orogeny in Northeast Brazil. In: Dallmeyer R.D., Lecorche J.P. (eds.). The west African orogens and circum-Atlantic correlatives, Springer-Verlag Berlin Heidelberg, p. 373-397. https://doi.org/10.1007/978-3-642-84153-8_16
- Cavalcante R., Medeiros V.C., Costa A.P., Sá J.M., Santos R.V., Rodrigues J.B., Dantas A.R., Nascimento M.A.L., Cunha, A.L.C. 2018. Neoproterozoic, Rhyacian and Neoproterozoic units of the Saquinho region, eastern Rio Piranhas-Seridó domain, Borborema Province (northeastern Brazil): implications for the stratigraphic model. *Journal of the Geological Survey of Brazil*, 1, 11-29. <https://doi.org/10.29396/jgsb.2018.v1.n1.2>
- Cerný P. 1989. Exploration strategy and methods for pegmatite deposits of tantalum. In: Moller P., Cerný P., Saupe F. (eds.). Lanthanides, tantalum, and niobium. New York: Springer-Verlag, p. 274-302. https://doi.org/10.1007/978-3-642-87262-4_13
- Cerný P., Meintzer R.E. 1988. Fertile granites in the Archean and Proterozoic fields of rare element pegmatites: crustal environment, geochemistry and petrogenetic relationships. In: Taylor R.P., Strong D.F. (eds.). Recent advances in the geology of granite-related mineral deposits. Canadian Institute of Mining and Metallurgy, Special Publication 39, 170-206.
- Costa A.P., Dantas A.R. 2014. Carta Geológica da Folha Lajes SB.24-X-D-VI, Estado do Rio Grande do Norte, Escala 1:100.000. Programa Geologia do Brasil, Recife, CPRM. Available on line at: <http://geosgb.cprm.gov.br/> (accessed on 26 December 2018).
- Costa A.P., Dantas A.R., Cavalcante R., Spisla A.L., Cunha A.L.C., Lima R.B. 2018. Projeto ARIM Seridó – Folhas SB.24-Z-B-II-1 e SB.24-Z-B-II-3 (partes) - Distrito de Bonfim: Estado do Rio Grande do Norte. Mapa Geológico-Geofísico, Escala 1:50.000. 1 mapa colorido, 75 x 74 cm. Avaliação dos Recursos Minerais do Brasil, Recife, CPRM.
- Dantas E.L. 1988. Mapeamento geológico da região de Florânia-RN. Graduation work, Departamento de Geologia, Universidade Federal do Rio Grande do Norte, Natal, 270 p.
- Dantas R.C., Dantas E.L., Oliveira C.G. 2014. Geoquímica e geocronologia U-Pb e Sm-Nd das rochas encaixantes arqueanas do depósito de W-Au Bonfim-RN, Faixa Seridó, Província Borborema. In: Congresso Brasileiro de Geologia, 47, 1914.
- Evensen N.M., Hamilton P.J., O’Nions R.K. 1978. Rare earth abundances in chondritic meteorite. *Geochimica et Cosmochimica Acta*, 42(8), 1199-1212. [https://doi.org/10.1016/0016-7037\(78\)90114-X](https://doi.org/10.1016/0016-7037(78)90114-X)
- Frost B.R., Barnes C.G., Collins W.J., Arculus R.J., Ellis D.J., Frost C.D. 2001. A geochemical classification for granitic rocks. *Journal of Petrology*, 42(11), 2033-2048. <https://doi.org/10.1093/petrology/42.11.2033>
- Harrison T.M., Watson E.B. 1984. The behavior of apatite during crustal anatexis: equilibrium and kinetic considerations. *Geochimica et Cosmochimica Acta*, 48(7), 1467-1477. [https://doi.org/10.1016/0016-7037\(84\)90403-4](https://doi.org/10.1016/0016-7037(84)90403-4)
- Hollanda M.H.B.M., Archanjo C.J., Bautista J.R., Souza L.C. 2015. Detrital zircon ages and Nd isotope compositions of the Seridó and Lavras da Mangabeira basins (Borborema Province, NE Brazil): evidence for exhumation and recycling associated with a major shift in sedimentary provenance. *Precambrian Research*, 258, 186-207. <https://doi.org/10.1016/j.precamres.2014.12.009>
- Hollanda M.H.B.M., Archanjo C.J., Souza L.C., Duny L., Armstrong R. 2011. Long-lived Paleoproterozoic granitic magmatism in the Seridó-Jaguaribe domain, Borborema Province–NE Brazil. *Journal of South American Earth Sciences*, 32(4), 287-300. <https://doi.org/10.1016/j.jsames.2011.02.008>
- Jardim de Sá E.F. 1984. Geologia da região Seridó: reavaliação de dados. In: Simpósio de Geologia do Nordeste, 11, 278-296.
- Jardim de Sá E.F. 1994. A Faixa Seridó (Província Borborema, NE do Brasil) e o seu significado geodinâmico na Cadeia Brasileira/Pan-Africana. PhD Thesis, Universidade de Brasília, Brasília, 803 p.
- Jardim de Sá E.F., Macedo M.H.F., Fuck R.A., Kawashita K. 1992. Terrenos proterozóicos na Província Borborema e a margem norte do Cráton São Francisco. *Revista Brasileira de Geociências*, 22(4), 472-480. <https://doi.org/10.25249/0375-7536.1991472480>
- Jardim de Sá E.F., Macedo M.H.F., Torres H.F., Kawashita K. 1988. Geochronology of metaplutonics and the evolution of supracrustal belts in the Borborema Province, NE Brazil. In: Congresso Latino-Americano de Geologia, 7, 49-62.
- Jardim de Sá E.F., Salim J. 1980. Reavaliação dos conceitos estratigráficos na região do Seridó (RN-PB). *Mineração e Metalurgia*, 80, 16-28.
- Ludwig, K.R. 2003. Isoplot 3.00 - A Geochronological Toolkit for Microsoft Excel. Berkeley Geochronology Center, Special Publication, 4.
- Luth W.C., Jahns R.H., Tuttle O.F. 1964. The granite system at pressures of 4 to 10 kilobars. *Journal of Geophysical Research*, 69(4), 759-773. <https://doi.org/10.1029/JZ069i004p00759>
- Maniar P.D., Piccoli P.M. 1989. Tectonic discrimination of granitoids. *Geological Society of America Bulletin*, 101(15), 635-643. [https://doi.org/10.1130/0016-7606\(1989\)101<0635:TDOG>2.3.CO;2](https://doi.org/10.1130/0016-7606(1989)101<0635:TDOG>2.3.CO;2)
- Medeiros V.C., Cavalcante R., Cunha A.L.C., Dantas A.R., Costa A.P., Brito A.A., Rodrigues J.B., Silva M.A. 2017. O furo estratigráfico de Riacho Fechado (Carris Novos/RN), domínio Rio Piranhas-Seridó (província Borborema, NE Brasil): procedimentos e resultados. *Estudos Geológicos*, 27(3), 3-44. <https://doi.org/10.18190/1980-8208/estudosgeologicos.v27n3p1-40>
- Medeiros V.C., Nascimento M.A.L., Galindo A.C., Dantas E.L. 2012. Augen gnaisses riacianos no Domínio Rio Piranhas-Seridó - Província Borborema, Nordeste do Brasil. *Geologia USP, Série Científica*, 12(2), 3-4. <https://doi.org/10.5327/Z1519-874X2012000200001>
- Nascimento M.A.L., Galindo A.C., Medeiros V.C. 2015. Ediacaran to Cambrian magmatic suites in the Rio Grande do Norte domain, extreme Northeastern Borborema Province (NE of Brazil): current knowledge. *Journal of South American Earth Sciences*, 58, 281-299. <https://doi.org/10.1016/j.jsames.2014.09.008>
- Paes V.J.C., Santos L.D., Tedeschi M.F., Bettiolo L.M. 2016. Avaliação do potencial do lítio no Brasil: área do Médio Rio Jequitinhonha, Nordeste de Minas Gerais: texto explicativo e mapas. Belo Horizonte, CPRM, 276 p.
- Pearce J.A., Harris N.B., Tindle A.G. 1984. Trace element discrimination diagrams for the tectonic interpretation of granitic rocks. *Journal of Petrology*, 25(4), 956-983. <https://doi.org/10.1093/petrology/25.4.956>
- Ruiz F.V., Della Giustina M.E.S., Oliveira C.G., Dantas E.L., Hollanda

- M.H.B. 2018. The 3.5 Ga São Tomé layered mafic-ultramafic intrusion, NE Brazil: insights into a Paleoproterozoic Fe-Ti-V oxide mineralization and its reworking during West Gondwana assembly. *Precambrian Research*, 326, 462-478. <https://doi.org/10.1016/j.precamres.2018.03.011>
- Santos E.J. 1996. Ensaio preliminar sobre terrenos e tectônica acrescionária na Província Borborema. In: Congresso Brasileiro de Geologia, 39, 47-50.
- Santos E.J., Brito Neves B.B. 1984. Província Borborema. In: Almeida F.F.M., Hasui Y. (eds.). *O pré-cambriano do Brasil*. São Paulo, Edgard Blucher, p. 123-186.
- Santos E.J., Brito Neves B.B. de, Van Schmus W.R., Oliveira R.G., Medeiros V.C. 2000. An overall view on the displaced terrane arrangement of the Borborema Province, NE Brazil. In: International Geological Congress, 31, CD-ROM.
- Selway J.B., Breaks F.W., Tindle A.G. 2005. A review of rare-element (Li-Cs-Ta) pegmatite exploration techniques for the Superior Province, Canada, and large worldwide tantalum deposits. *Exploration and Mining Geology*, 14(1-4), 1-30. <https://doi.org/10.2113/gsemg.14.1-4.1>
- Souza Z.S. 1991. *Petrogénese des metagranitoides du Complexe de Caicó, Province Borborema (Etat du Rio Grande do Norte, Brésil)*. MSc Dissertation, CAESS, Université de Rennes, Rennes, 87 p.
- Souza Z.S., Kalsbeek F., Deng X-D., Frei R., Kokfelt T.F., Dantas E.L., Li J-W., Pimentel M.M., Galindo A.C. 2016. Generation of continental crust in the northern part of the Borborema Province, northeastern Brazil, from Archean to Neoproterozoic. *Journal of South American Earth Sciences*, 68, 68-96. <https://doi.org/10.1016/j.jsames.2015.10.006>
- Souza Z.S., Martin H., Peucat J.-J., Jardim de Sá E.F., Macedo M.H.F. 2007. Calc-alkaline magmatism at the Archean and Proterozoic transition: the Caicó complex basement (NE Brazil). *Journal of Petrology*, 48(11), 2149-2185. <https://doi.org/10.1093/petrology/egm055>
- Souza Z.S., Souza L.C., Vilalva F.C.J., Cruz L.B., Ribeiro C.V.A., Oliveira A.L.S., Cruz J.A., Araújo J.B.P. 2018. Magmatismo peraluminoso sintectônico à deformação tangencial em Jardim do Seridó/RN, NE do Brasil. In: Congresso Brasileiro Geologia, 49.
- Sylvester P.J. 1989. Post-collisional alkaline granites. *The Journal of Geology*, 97(3), 261-280.
- Taylor S.R., McLennan S.M. 1985. *The continental crust: its evolution and composition*. Oxford: Blackwell Scientific, 312p. <https://doi.org/10.1002/gj.3350210116>
- Thiéblemont D., Cabanis B. 1990. Utilisation d'un diagramme (Rb/100)-Tb-Ta pour la discrimination géochimique et l'étude pétrogénétique des roches magmatiques acides. *Bulletin de la Société Géologique de France*, 6(1), 23-35. <https://doi.org/10.2113/gssgfbull.VI.1.23>
- Tuttle O. F., Bowen N.L. 1958. Origin of granite in the light of experimental studies in the system: NaAlSi₃O₈. *Geological Society of America*, 74. <https://doi.org/10.1130/MEM74-p1>
- Van Schmus W.R., Brito Neves B.B. de, William I.S., Hackspacher P.C., Fetter A.H, Dantas E.L., Babinski M. 2003. The Seridó Group of NE Brazil, a late Neoproterozoic pre- to syn-collisional basin in West Gondwana: insights from SHIRIMP U-Pb detrital zircons ages and Sm-Nd crustal residence (TDM) ages. *Precambrian Research*, 127(4), 287-386. [https://doi.org/10.1016/S0301-9268\(03\)00197-9](https://doi.org/10.1016/S0301-9268(03)00197-9)
- Van Schmus W.R., Brito Neves B.B., Hackspacher P.C., Babinski M. 1995. U-Pb and Sm-Nd geochronologic studies of the Eastern Borborema Province, Northeast Brazil: initial conclusions. *Journal of South American Earth Sciences*, 8(3-4), 267-288. [https://doi.org/10.1016/0895-9811\(95\)00013-6](https://doi.org/10.1016/0895-9811(95)00013-6)
- Wones D.R. 1989. Significance of the assemblage titanite+ magnetite+ quartz in granitic rocks. *American Mineralogist*, 74(7-8), 744-749.